

## Inversion Point and Internal Volume of Pressurized Nonlinearly Elastic Tube

Lukáš Horný<sup>1\*</sup>, Zdeněk Petřivý<sup>1</sup>

<sup>1</sup> Faculty of Mechanical Engineering, Czech Technical University in Prague, Technická 4, Prague, 160 00, Czech Republic

\*Corresponding author: Lukáš Horný, [Lukas.horny@fs.cvut.cz](mailto:Lukas.horny@fs.cvut.cz)

### Abstract

The mechanical response of a hollow circular cylinder to internal pressure represents an important theoretical model which can be helpful in the design of tubular structures, and in the biomechanical research of tissues like arteries. It has been shown that arteries *in vivo*, in addition to pressure loading, sustain significant axial extension. It is manifested as a retraction that is observed when they are excised from a body. Previous research has shown that the axial prestretch ensures that the longitudinal motion of arteries is negligible under physiological conditions. The magnitude of the axial prestretch at which a tube does not change its length during pressurization, is referred to as the inversion point, because at this point mechanical response changes from pressure-induced elongation to pressure-induced shortening. In the present paper, another property observed when a nonlinear elastic tube is inflated at a constant axial load is studied. It is shown that at axial prestretching corresponding to the inversion point, when a tube exhibits no axial movement, the maximum internal volume of the pressurized tube is attained. This property is shown for thin-walled tubes made from material that is characterized with Mooney-Rivlin and Gent strain energy density function. Differences in the inflation-extension response obtained for Gent's material, and for the human abdominal aorta that is considered to be anisotropic and is described with exponential strain energy density, are studied in the paper. To the best of our knowledge, our study is the first showing that the maximum internal volume of the inflated tube is intimately linked with its axial prestretch.

**Keywords:** Axial prestretch, hyperelasticity, inflation-extension behaviour, maximum volume, pressure, thin-walled tube.

## 1. Introduction

The mechanical response of a nonlinearly elastic hollow circular cylinder to internal pressure represents an important theoretical model which can be helpful when studying the behaviour of tubular tissues like arteries or veins [1-3]. As well as biomechanical examples, elastomer pipes used in a variety of industrial applications can also be modelled as nonlinear cylindrical tubes loaded by internal pressure.

It has been shown that arteries, in addition to pressure loading, sustain significant axial extension [3-10]. This is manifested as a retraction that is observed in autopsy or surgery, when arteries are excised from a body. It follows that they have to be considered as longitudinally prestretched and the specific value of the prestretch is determined as a ratio of in situ length to ex situ length. The magnitude of the prestretch depends on anatomical location (see works by Horný and colleagues for detailed description of the prestretch in the human abdominal aorta and carotid arteries [3, 6-8], and Kamenskiy et al. for results obtained in popliteal artery [9,10], and Schulze-Bauer et al. for the prestretch measured in iliac arteries [11]). Since age-related changes significantly affect our cardiovascular system, the prestretch depends also on age [3,6-12].

The fact that arteries are axially prestretched has important consequences for their mechanical response. Theoretical analysis based on thin-walled, as well as thick-walled tube models, and also ex vivo experiments, have shown that it is axial prestretch which ensures that the longitudinal motion of the aorta is almost negligible under physiological conditions [3,13-15]. Originally, it was assumed that almost zero axial deformation during pressure pulse transmission, is a consequence of significant tethering (attachment to surrounding tissue) [13]. At present we would rather say that the longitudinal immobility of arteries results from a biological tuning that couples constitutive properties, internal structure and the physiological range of arterial loading.

To be more specific, it was found that a typical in vitro inflation behaviour of an artery, held at constant length, is such that there is a value of the axial stretching, above which the force–pressure relationship creates an increasing curve, and under a stretch smaller than this value, the force–pressure relationship is decreasing [14-16]. On the other hand, when constant force is considered instead of constant axial deformation (which can, for example, be carried out by hanging a weight during inflation of vertically oriented tube), pressurization experiments have shown that for small values of the load the arteries elongate, whereas at bigger values of axial load, they shorten during pressurization [11,17-18]. It is generally accepted that the in vivo value of this prestretch is exactly the value under which an artery neither shortens nor elongates in the pressure cycle. This value is referred to by some authors as the *inversion stretch*, or the stretch at *inversion point*, because it creates a boundary in the mechanical response of the tube. At this point, which, in what follows will be denoted as  $\lambda_z^{inv}$ , the response changes from pressure-induced elongation to pressure-induced shortening [11,17-18].

In the present paper we would like to demonstrate another interesting property which can be observed when a nonlinear elastic tube is inflated at a constant axial load. It will be shown that at axial prestretching corresponding to the inversion point, when no axial movement is exhibited during inflation, the maximum internal volume of the pressurized tube is attained. This property will be demonstrated by means of an analytical model based on a thin-wall assumption, and adopting Mooney-Rivlin and Gent's strain energy density function, which are known from elastomer elasticity [12,19-21]. Results obtained with anisotropic elastic potential, corresponding to the human abdominal aorta [22], will suggest that a phenomenon of volume maximization also takes place in the inflation-extension response of the human arteries, but the inversion in axial response can no longer be understood as a global property. To the best of our knowledge, our study is the first showing that the axial prestretch can optimize inflation volume. This feature may be found valuable when one considers cylindrical tubes as pressurized containers that feed some type of medium.

## 2. Methods

### 2.1 Kinematics of inflation–extension response

In our study, we are focused on the mechanics of a circular cylindrical tube which is in an axial direction loaded by a weight in order to induce initial axial extension,  $\lambda_Z^{ini}$ , referred to as axial prestretch. When the tube is prestretched, loading by internal pressure follows. In the reference configuration, the geometry of the tube is in cylindrical polar coordinates  $(R, \Theta, Z)$  defined by

$$R_i \leq R \leq R_o, \quad 0 \leq \Theta \leq 2\pi, \quad 0 \leq Z \leq L, \quad (1)$$

where  $R_i$ ,  $R_o$ , and  $L$  denote inner radius, outer radius and length of the tube, respectively. It is assumed that the deformation of the tube is expressed by the equations

$$r^2 - r_i^2 = \lambda_Z^{-1} (R^2 - R_i^2), \quad \theta = \Theta, \quad z = \lambda_Z Z, \quad (2)$$

where  $(r, \theta, z)$  are cylindrical polar coordinates in the deformed configuration, and  $r_i$  denotes the inner radius of the deformed tube. The equations (2) express the fact that the tube uniformly inflates and extends, and that it does not twist. Hence the deformation gradient  $\mathbf{F}$  is diagonal and can be in the matrix form written as  $\mathbf{F} = \text{diag}[\lambda_R, \lambda_\Theta, \lambda_Z]$ . The material of the tube is assumed to be incompressible thus  $\det(\mathbf{F}) = \lambda_R \lambda_\Theta \lambda_Z = 1$ . Particular value of the circumferential stretch is given by  $\lambda_\Theta = r/R$ . When  $\lambda_Z$  is known, radial stretch  $\lambda_R$  can be obtained by means of the incompressibility condition. Further discussion of the described kinematics can be found in [1,17,30,40-41].

### 2.2 Constitutive models

It is assumed that the tube is made from nonlinearly elastic material characterized with an elastic potential  $W$ . For such a material, a constitutive equation can be written in the form of (3). Here  $\boldsymbol{\sigma}$  is the Cauchy stress tensor,  $\mathbf{I}$  denotes second-order unit tensor, and  $p$  plays a role of the Lagrangean multiplier which is determined by means of a force boundary condition.

$$\boldsymbol{\sigma} = \frac{\partial W}{\partial \mathbf{F}} \mathbf{F}^T - p \mathbf{I} \quad (3)$$

*Elastomer tube.* The simplest form of the strain energy density  $W$  is a classical neo-Hookean model

$$W = \frac{\mu}{2} (I_1 - 3). \quad (4)$$

Here  $\mu$  is the stress-like material parameter, which at infinitesimal strains corresponds to the shear modulus, and  $I_1$  is the first principal invariant of the right Cauchy-Green strain tensor  $\mathbf{C}$ ,  $\mathbf{C} = \mathbf{F}^T \mathbf{F}$ . This model however has quite limited applicability when confronted with typical elastomer experimental data. A simple extension of (4) by means of adding linear term with the second invariant of  $\mathbf{C}$ ,  $I_2$ , gives

$$W = \frac{\mu}{2} (I_1 - 3) + \frac{\nu}{2} (I_2 - 3), \quad (5)$$

which is referred to as the Mooney-Rivlin model. Similarly to  $\mu$ ,  $\nu$  is a stress-like parameter. Although (5) includes a new independent variable, it also fails to accurately describe stiffening of macromolecular materials observed at large strains.

One of the simplest models that is known to be capable of reproducing the nonlinear mechanical behaviour of elastomers, is the Gent's strain energy density function [19-21, 23, 30]. This model is also sometimes used to describe soft tissues (including arterial walls) when their mechanical behaviour is modelled as isotropic [12, 30]. Its particular form is

$$W = -\frac{\mu J_m}{2} \ln \left( 1 - \frac{I_1 - 3}{J_m} \right). \quad (6)$$

Here  $\mu$  is the stress-like material parameter, which at infinitesimal strains corresponds to the shear modulus, and  $J_m$  is the dimensionless parameter modulating nonlinear behaviour of the material. Gent's material model belongs to the class of so-called limiting chain extensibility models, which means that admissible deformations are restricted to a certain subset in the space of all deformations. It is clear from (6) that admissible deformation has to satisfy  $I_1 < J_m + 3$ . Due to this fact, stress-strain curves obtained for Gent's material exhibit significant large strain stiffening when  $I_1$  approaches  $J_m + 3$ .

*Human abdominal aorta.* To show whether axial prestretch may lead to a maximization of the internal volume of an inflated artery, a constitutive model describing the mechanical response of the human abdominal aorta is adopted from [22]. Its specific form is expressed in (7)

$$W = \frac{c_0}{2} (I_1 - 3) + \sum_{j=4,6} \frac{k_1}{2k_2} \left( e^{k_2(I_j - 1)^2} - 1 \right). \quad (7)$$

The model (7) splits stored energy into two portions. The first corresponds to a contribution represented by the isotropic component of the artery wall, and in (7) is expressed with the Neo-Hookean term. Typically, the mechanical response of elastic fibres, smooth muscle cells in their passive state, and the response of other proteoglycans is assumed to be captured by this term [22, 24, 25].

The nonlinear part of (7), that is a sum of exponential functions, is interpreted as a contribution of collagen fibres which are generally accepted to be responsible for the large strain stiffening observed in the mechanical response of arteries. It is assumed that collagen fibres are arranged into two families of helically oriented bundles of fibres, which are symmetrically disposed with respect to circumferential axis by angle  $\pm\beta$ . Thus the model (7) regards the artery wall as a continuum with two preferred directions that are in polar cylindrical coordinates  $(R, \Theta, Z)$  characterized with unit material vectors  $\mathbf{M} = (0, \cos(\beta), \sin(\beta))^T$ , and  $\mathbf{N} = (0, \cos(-\beta), \sin(-\beta))^T$ . It follows from the existence of preferred directions, that additional deformation invariants, induced by an anisotropy, can be defined. The model (7) employs  $I_4$  and  $I_6$  that are obtained as

$$I_4 = \mathbf{M} \cdot \mathbf{C} \mathbf{M} = \lambda_\Theta^2 \cos^2(\beta) + \lambda_Z^2 \sin^2(\beta), \quad I_6 = \mathbf{N} \cdot \mathbf{C} \mathbf{N} = \lambda_\Theta^2 \cos^2(-\beta) + \lambda_Z^2 \sin^2(-\beta). \quad (8)$$

Thus (7) includes four material parameters  $c_0$ ,  $k_1$ ,  $k_2$ , and  $\beta$ . The model (7) was introduced by G. A. Holzapfel, T. C. Gasser, and R. W. Ogden in [24] and is now frequently referred to as the HGO model. Later on, the authors have modified this model to take into account the imperfect directional arrangement of fibres, by considering their dispersion around preferred direction [25]. Some authors also use (7) in the form that incorporate more than two preferred directions [34-37]. Further information about anisotropic elasticity can be found for instance in [41, 42].

It is worth noting at this point that (7) is only a model, and although it has a clear structural interpretation, readers should not confuse it with the true internal architecture of our arteries. Nevertheless, we are here focused on the effect of axial prestretch and details of arterial histology are beyond our scope.

### 2.3 Equilibrium of a tube during simultaneous inflation and extension

The equilibrium equations in a local form can be, under absence of body and inertial forces, compactly written as  $\text{div}(\boldsymbol{\sigma}) = 0$ . Due to circular symmetry, axial uniformity, and absence of shear stresses, the only component that is not satisfied trivially is

$$\frac{d\sigma_{rr}}{dr} + \frac{\sigma_{rr} - \sigma_{\theta\theta}}{r} = 0, \quad (9)$$

which expresses an equilibrium in a radial direction. Boundary conditions that are considered in our problem are  $\sigma_{rr}(r_i) = -P$ ,  $\sigma_{rr}(r_o) = 0$ . Using boundary conditions and constitutive equations for incompressible material written in the form of

$$\sigma_{\theta\theta} - \sigma_{rr} = \lambda_{\Theta} \frac{\partial \hat{W}}{\partial \lambda_{\Theta}}, \quad \sigma_{zz} - \sigma_{rr} = \lambda_z \frac{\partial \hat{W}}{\partial \lambda_z}, \quad (10)$$

(9) can be integrated to (11)

$$P = \int_{r_i}^{r_o} \lambda_{\Theta} \frac{\partial \hat{W}}{\partial \lambda_{\Theta}} \frac{dr}{r}. \quad (11)$$

Here  $\hat{W}$  denotes  $W$  after  $\lambda_R$  is substituted with  $1/(\lambda_{\Theta}\lambda_z)$ . Details of the derivation can be found, for instance, in [38, 39]. Further substitution of  $r$  by  $\lambda_{\Theta}$ , with a help of  $r = \lambda_{\Theta}R$  and  $dr = R/(1 - \lambda_{\Theta}^2\lambda_z)d\lambda_{\Theta}$ , gives (12)

$$P = \int_{\lambda_{\Theta o}}^{\lambda_{\Theta i}} \frac{\partial \hat{W}}{\partial \lambda_{\Theta}} \frac{d\lambda_{\Theta}}{\lambda_{\Theta}^2\lambda_z - 1}, \quad (12)$$

where notations  $\lambda_{\Theta i} = r_i/R_i$ , and  $\lambda_{\Theta o} = r_o/R_o$  are introduced. In this study, we will restrict our attention to a thin-walled approximation, which is obtained from (12) by means of the mean value theorem. Volume preservation condition is used to derive  $\lambda_{\Theta i} - \lambda_{\Theta o} = \varepsilon\lambda_{\Theta}^{-1}\lambda_z^{-1}(\lambda_{\Theta}^2\lambda_z - 1)$ , where the parameter  $\varepsilon = H/R_i = (R_o - R_i)/R_i$  is considered to be small. The final equation, that expresses how to compute internal pressure when the deformation and constitutive properties of the thin-walled cylindrical membrane tube are given, is in (13),

$$P = \frac{\varepsilon}{\lambda_{\Theta}\lambda_z} \frac{\partial \hat{W}}{\partial \lambda_{\Theta}}. \quad (13)$$

Further details of the used approach can be found for instance in [40-42].

Since our attention is aimed at the effect of axial prestretching, the axial equilibrium of the pressurized cylindrical tube will also be employed. It can be written in the following way

$$F_{red} + \pi r_i^2 P = 2\pi \int_{r_i}^{r_o} \sigma_{zz} r dr. \quad (14)$$

This equation expresses that the reduced axial force,  $F_{red}$ , which is the force inducing axial prestretch and pressure, acting at closed ends of the tube, are balanced by axial stress  $\sigma_{zz}$ . With the help of (10)<sub>2</sub>, boundary conditions,  $2r = d(r^2)/dr$ , and integration *per partes*, (14) can be transformed to the following form

$$F_{red} = \pi \int_{r_i}^{r_o} \left( 2\lambda_z \frac{\partial \hat{W}}{\partial \lambda_z} - \lambda_\Theta \frac{\partial \hat{W}}{\partial \lambda_\Theta} \right) r dr. \quad (15)$$

All necessary steps are explained in detail, for example, in [38, 39]. Now, similarly to (11) and (12), the independent variable in the equation (15) is changed from  $r$  to  $\lambda_\Theta$ . This is obtained by the same steps as described above for (11), and by using (2)<sub>1</sub> written in the form  $R^2 = (\lambda_z r_i^2 - R_i^2)/(\lambda_\Theta^2 \lambda_z - 1)$ . Reduced axial force is then given as

$$F_{red} = \pi R_i^2 (\lambda_\Theta^2 \lambda_z - 1) \int_{\lambda_{\Theta_0}}^{\lambda_{\Theta_1}} \left( 2\lambda_z \frac{\partial \hat{W}}{\partial \lambda_z} - \lambda_\Theta \frac{\partial \hat{W}}{\partial \lambda_\Theta} \right) \frac{\lambda_\Theta}{(\lambda_\Theta^2 \lambda_z - 1)^2} d\lambda_\Theta. \quad (16)$$

The final step is again application of the mean value theorem. It results in (17), that in the case of the thin-walled cylindrical membrane approximates  $F_{red}$ ,

$$F_{red} = \pi R_i^2 \varepsilon \left( 2 \frac{\partial \hat{W}}{\partial \lambda_z} - \frac{\lambda_\Theta}{\lambda_z} \frac{\partial \hat{W}}{\partial \lambda_\Theta} \right). \quad (17)$$

### 3. Inversion in axial deformation of the pressurized thin-walled tube

As was mentioned in the introduction, an axially prestretched tube may exhibit inversion in its axial response to internal pressure. It means that the tube, which is prestretched by  $F_{red}$  to  $\lambda_z^{mi}$  and subsequently loaded by pressure  $P$ , may show pressure-induced elongation ( $\lambda_z$ - $P$  curve is increasing), pressure-induced shortening ( $\lambda_z$ - $P$  curve is decreasing), or may withstand pressurization without any change of its length. In the latter case, the tube is prestretched exactly to  $\lambda_z^{mi} = \lambda_z^{inv}$  at which the length of the tube is independent of applied pressure. This is of course not a general feature of all tubes. R. W. Ogden and C. A. J. Schulze-Bauer studied this property in their work [17], and derived a condition that the strain energy density function has to satisfy in order to exhibit axial inversion in the mathematical model based on (13) and (17).

This condition can be obtained from traces of  $F_{red} = constant$  in  $\lambda_\Theta$ - $\lambda_z$  plane. The fact that the length of the tube does not change during pressurization means that  $\lambda_z$  is independent of  $\lambda_\Theta$ , and the condition of inversion point is given as  $\partial \lambda_z / \partial \lambda_\Theta = 0$ . In order to express it by means of the strain energy  $W$ , one can employ a derivative of a function given implicitly with  $F_{red}$  as an equation coupling  $\lambda_\Theta$  and  $\lambda_z$ . It results in

$$\lambda_\Theta \frac{\partial^2 \hat{W}}{\partial \lambda_\Theta^2} + \frac{\partial \hat{W}}{\partial \lambda_\Theta} - 2\lambda_z \frac{\partial^2 \hat{W}}{\partial \lambda_\Theta \partial \lambda_z} = 0. \quad (18)$$

This equation can be found in [17, 30, 40]. When a root of (18) independent of  $\lambda_\Theta$  is found, it follows that given  $W$  exhibits inversion point.

It is easy to show that neo-Hookean strain energy (4) does not exhibit inversion point because the root of (18) is  $\lambda_\theta^{-2}$  in this case. However, the Mooney-Rivlin model (5) gives  $\sqrt{(\mu/\nu)}$  which is independent of  $\lambda_\theta$ . Thus Mooney-Rivlin strain energy density seems to be the simplest model that exhibits inversion point. Figure 1 depicts this property by means of the numerical solution of (13) and (17) for  $\mu/\nu = 2$ . A similar graph created for neo-Hookean model can, for interested readers, be found in [29] (cf. Figure 2 in [29]).

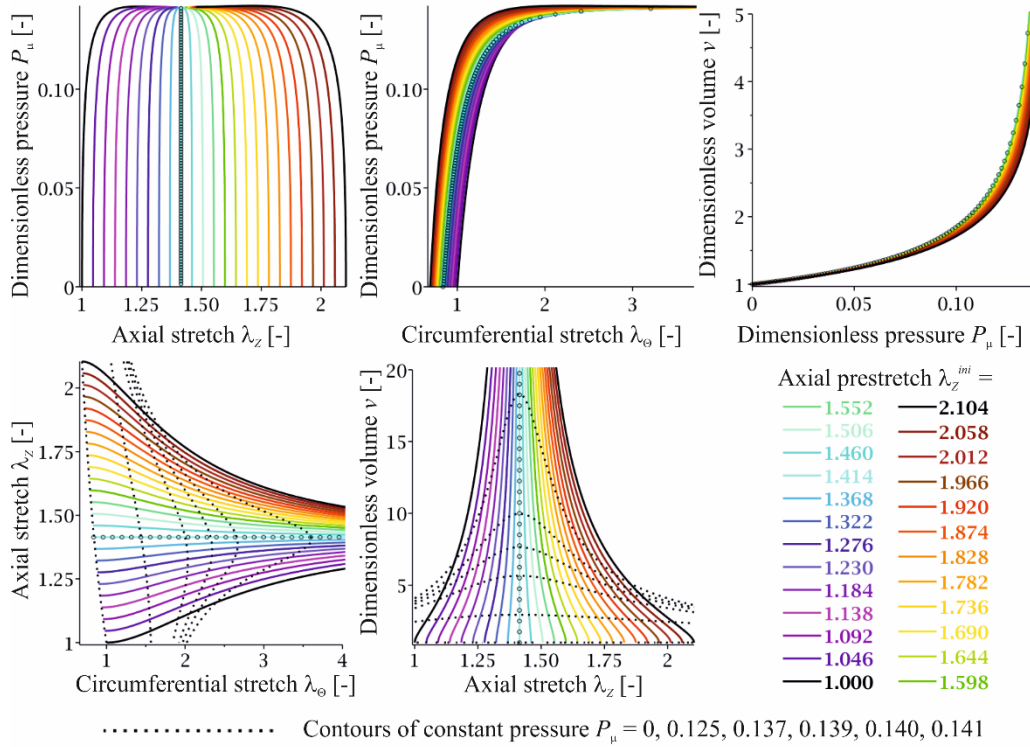


Figure 1. Numerical results of the simulation of the pressurization of an axially prestretched thin-walled tube with the elastic potential modelled by Mooney-Rivlin strain energy density with  $\mu/\nu = 2$ . Inversion in the axial response is depicted with a line created by open black circles at position  $\lambda_z = \sqrt{2}$ .

Existence of the inversion point in Gent's model has been thoroughly studied in [30, 40]. In this case, the equation (18) gives a root independent of the circumferential stretch and it applies that  $\lambda_z^{inv} = \sqrt{(1 + J_m/3)}$ . Pressurization of an axially prestretched tube with the strain energy density corresponding to the Gent model is illustrated in Figure 2 for  $J_m = 3$ . The Gent model is in [30, 40] compared with Fung-Demiray strain energy density

$$W = \frac{\mu}{2b} \left( e^{b(l-3)} - 1 \right), \quad (19)$$

which has been in various papers used to model the mechanical properties of biological tissues, and may be understood as the exponential counterpart of the Gent model. It is shown in [30, 40] that (18) does not have a solution independent of  $\lambda_\theta$  for (19) and thus the Fung-Demiray model does not show the inversion point in its inflation-extension response (cf. Figure 1 in [29]).

With regard to the anisotropic strain energy density function (7), we tried to solve (18) with the help of the computer algebra system Maple (version 2019) because the resulting equation was very complicated. However, we were not able to find  $\lambda_z$  that would be satisfied (18) independently of  $\lambda_\theta$ . It shows that the

inversion point in the model (7) does not exist. Inflation-extension response of the model (7) with material parameters corresponding the human abdominal aorta is depicted in Figure 3 (details of the simulation are described in the following).

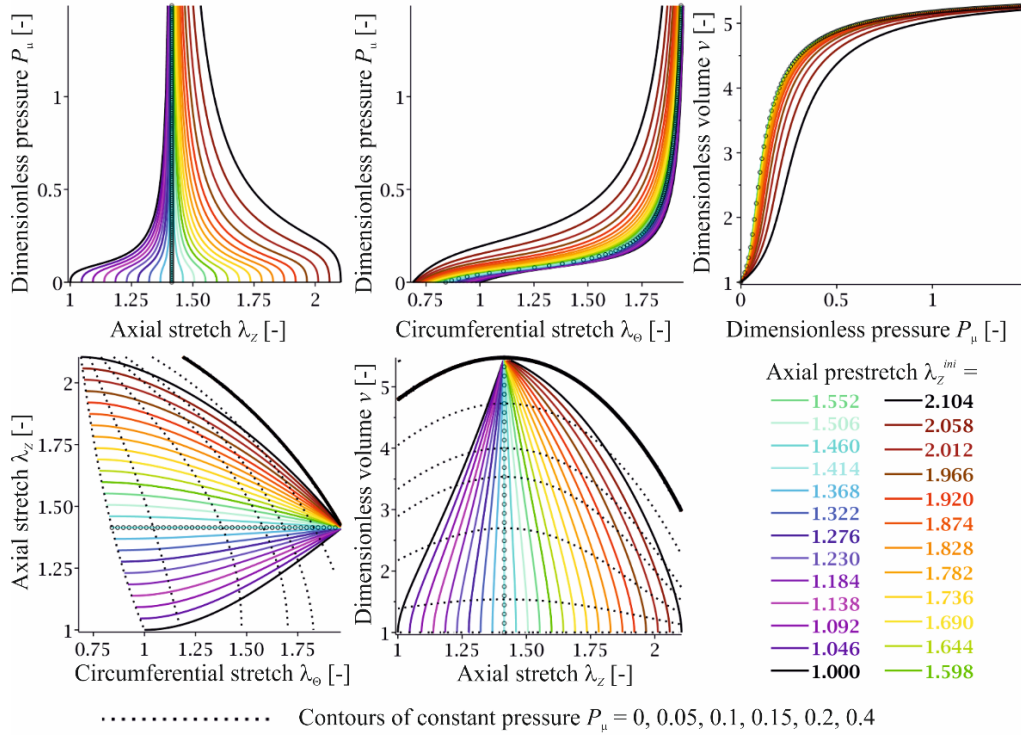


Figure 2. Numerical results of the simulation of the pressurization of an axially prestretched thin-walled tube with the elastic potential modelled by Gent's strain energy density with  $J_m = 3$ . Inversion in the axial response is depicted with line created by open black circles at position  $\lambda_z = \sqrt{2}$ .

#### 4. Internal volume of the axially prestretched thin-walled tube

Many pressure vessels serve as conduits for some medium. This is also the case with our arteries. With every pulse, the aorta accommodates blood ejected from the heart that is under physiological conditions almost constant at a short-time scale. From this point of view, it seems to be interesting to pose the question as to how does the axial prestretch affect internal volume that an inflated tube has.

Instead of absolute volume, we will restrict our attention to dimensionless volume ratio of deformed to reference internal volume

$$v = \frac{\pi r_i^2 l}{\pi R_i^2 L} = \lambda_\theta^2 \lambda_z, \quad (20)$$

where  $l$  denotes a deformed length of the inflated tube, and  $(20)_3$  is used because we work with a thin-wall approximation.

Now our particular question is: Does a certain value of the prestretch exist, so that a tube, pressurized at this prestretch, attains maximal internal volume? We chose a similar approach as in the case of a derivation of the condition (18). However, now  $\partial v / \partial \lambda_Z = 0$  is not expressed by means of  $F_{red} = constant$ , but with a help of  $P = constant$ . It is because our objective is, in fact, to find  $\lambda_Z$  that maximizes  $v$  at a given pressure. What follows is a standard use of an implicit function theorem as in the above case. Before doing so,  $\lambda_\Theta$  is in (13) substituted from (20),  $\lambda_\Theta = \sqrt{v / \lambda_Z}$ . Thus overall procedure can be expressed as

$$\frac{\partial}{\partial \lambda_Z} \left[ \frac{\varepsilon}{\lambda_\Theta \lambda_Z} \frac{\partial \hat{W}}{\partial \lambda_\Theta} \right]_{\lambda_\Theta = \sqrt{v / \lambda_Z}} = 0. \quad (21)$$

We will omit here specific forms of equations obtained by (21) for the material models discussed above, because particular expressions are rather complicated. However, (21) gives the same values of  $\lambda_Z$  as (18), when independency of  $v$  is required. Thus a neo-Hookean model has no optimal axial prestretch for a pressurized tube, in contrast to the Mooney-Rivlin model that gives maximum volume of the pressurized tube when it is prestretched to  $\lambda_Z^{ini} = \lambda_Z^{inv} = \sqrt{(\mu / \nu)}$ . Similarly, a tube made from a material that corresponds to the Gent strain energy density, exhibits maximum inflation volume when prestretched to  $\lambda_Z^{ini} = \lambda_Z^{inv} = \sqrt{(1 + J_m / 3)}$ . Finally for exponential models (7) and (19), we did not receive any constant value of the axial prestretch, i.e. independent of applied pressure, under which a tube would be inflated to maximum volume.

## 5. Simulation of the inflation and extension of a thin-walled tube

In order to demonstrate in detail how axial prestretch affects the inflation-extension behaviour of a tube, previous results will be completed with a numerical simulation of the mechanical response obtained by means of a solution of (13) and (17) for Mooney-Rivlin, Gent, and HGO model.

A prediction of inflation-extension response is obtained in two steps. First, axial prestretch of the tube is induced by assigning  $\lambda_Z = \lambda_Z^{ini}$  at zero pressure. In this step, the system (13, 17) is used to compute  $F_{red}$  necessary to pre-elongate the tube. Simultaneously the initial circumferential stretch  $\lambda_\Theta^{ini}$  is obtained. The second step differs depending on the material model. In case of Mooney-Rivlin strain energy density, the system (13, 17) is solved for unknown  $\lambda_Z$  and  $P$  with  $F_{red}$  and  $\lambda_\Theta$  being assigned. It is due to limiting value of the pressure in the Mooney-Rivlin response (see Figure 1). In the case of the Gent model and HGO, (13, 17) are solved for unknown  $\lambda_\Theta$  and  $\lambda_Z$  whereas  $P$  and  $F_{red}$  are assigned.

Calculations were carried out for  $\mu / \nu = 2$  (Mooney-Rivlin),  $J_m = 3$  (Gent), and results are presented in dimensionless form in these cases ( $P_\mu = P / \mu$ ). Parameter  $\varepsilon$  was considered to be 0.1. The values of the material parameters for the human abdominal aorta were chosen from [22] and correspond to a 38 year old male donor (denoted in [22] as M38). Specific values for parameters and geometry are listed in Table 1. All computations were carried out with a help of the computer algebra system, Maple (version 2019). A procedure of solving equations was based on *fsolve* command.

Table 1 Material parameters and geometry adopted from [22].

| ID in [22] | $\mu$<br>[kPa] | $k_1$<br>[kPa] | $k_2$<br>[-] | $\beta$<br>[°] | $R_i$<br>[mm] | $H$<br>[mm] |
|------------|----------------|----------------|--------------|----------------|---------------|-------------|
| M38        | 24.39          | 19.28          | 3.216        | 41.60          | 5.3           | 1.22        |

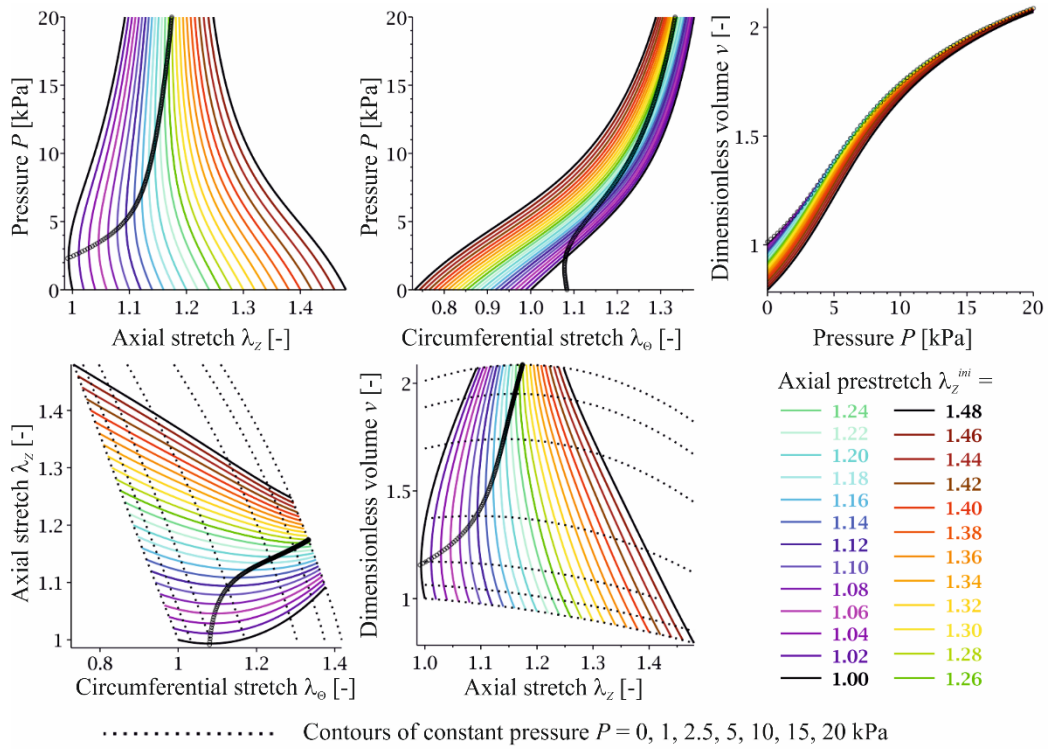


Figure 3. Numerical results of the simulation of the pressurization of axially prestretched thin-walled tube with the elastic potential corresponding to the human abdominal aorta modelled by (7) with parameters  $\mu = 24.39$  kPa,  $k_1 = 19.28$  kPa,  $k_2 = 3.216$ ,  $\beta = 41.6^\circ$ , and  $R_i = 5.3$  mm,  $H = 1.22$  mm (sample M38 in [22]). Points satisfying  $\partial\lambda_z/\partial\lambda_\theta = 0$  and  $\partial v/\partial\lambda_z = 0$  are depicted with open black circles. Black circles in  $\lambda_z$ - $P$  suggest that for  $P < 2.5$  kPa the prestretch determined from  $\partial\lambda_z/\partial\lambda_\theta = 0$  (and as well as from  $\partial v/\partial\lambda_z = 0$ ) satisfies  $\lambda_z^{ini} < 1$ .

## 6. Results of the simulation

Figure 1, 2, and 3 display numerical results for Mooney-Rivlin, Gent, and HGO models, respectively. Responses obtained at different values of the prestretch are distinguished by a colour. All figures have the same structure. Particularly, in the upper row the first panel shows  $\lambda_z$ - $P$  response, the second  $\lambda_\theta$ - $P$ , and the third  $P$ - $v$ . The lower row shows traces of the inflation-extension simulation in  $\lambda_\theta$ - $\lambda_z$  and  $\lambda_z$ - $v$  planes. In these planes, contours of  $P = \text{constant}$  are also presented, and it is worth remembering that inflation-extension traces are in fact contours of  $F_{red} = \text{constant}$ . Points that correspond to  $\partial\lambda_z/\partial\lambda_\theta = 0$  (axial inversion) and  $\partial v/\partial\lambda_z = 0$  (volume maximization) are indicated by open black circles.

Results clearly show that in Figure 1 and 2, there is a value of the prestretch under which pressure-induced elongation inverts to pressure-induced shortening. For numerical values specified above, this happens just at  $\lambda_Z^{inv} = \sqrt{2}$  and axial inversion creates a line that is perpendicular to horizontal ( $\lambda_Z$ - $P$ ,  $\lambda_Z$ - $v$ ) or vertical ( $\lambda_\Theta$ - $\lambda_Z$ ) axis.

Some aspects of the inflation-extension response obtained under different values of the prestretch have already been more or less discussed in various papers [3, 17, 29-33]. However, to the best of our knowledge, a property depicted in  $P$ - $v$  panels of Figure 1 and 2, has not, as yet, attracted scientific attention. These results show, in accordance with (21), that the maximum internal volume of a pressurized tube, made from a material that is modelled by Mooney-Rivlin and Gent elastic potential, is attained if the tube is axially prestretched to  $\lambda_Z^{ini} = \lambda_Z^{inv}$ .

This property is also well documented in  $\lambda_Z$ - $v$  panels (Figure 1 and 2). They display  $v = v(\lambda_Z)$  with an effect of the pressure illustrated by means of contours of constant  $P$ . Maximization of the volume is obvious from a fact that the line created with black empty circles intersects dotted curves of constant pressure in their peaks which correspond to maximum  $v$ .

One might expect that maximum volume inside a pressurized tube could be attained under a condition of maximal radial distension. However, it is not true, as documented in  $\lambda_\Theta$ - $\lambda_Z$  panels of Figure 1 and 2. Contours of a constant pressure, which are depicted with dotted curves, do not intersect line of  $\lambda_Z^{inv}$  at maximal  $\lambda_\Theta$ . It is clearly visible especially for low pressures.

An application of the volume maximization by axial prestretching could be the prestretch found in our arteries. In the introduction, it was mentioned that elastic arteries are significantly axially prestretched [3-10]. A hypothesis that may be derived from the results presented above, is that if arteries are prestretched to  $\lambda_Z^{ini} = \lambda_Z^{inv}$ , the volume accommodated in one pressure pulse will always be maximal, irrespective of the pressure that is used to inflate the artery.

Figure 3 summarizes results obtained in the simulation of the inflation-extension behaviour of the human abdominal aorta. Maximum volume trajectory,  $\partial v / \partial \lambda_Z = 0$ , is again depicted with empty black circles and it coincides with axial inversion determined from  $\partial \lambda_Z / \partial \lambda_\Theta = 0$ . It is clear, however, that there is a significant difference between (5) and (6) on the one side, and (7) on the other side. In contrast to Mooney-Rivlin and Gent, HGO model does not exhibit  $\lambda_Z^{inv}$  as the vertical line in  $\lambda_Z$ - $P$  graph and horizontal line in  $\lambda_\Theta$ - $\lambda_Z$ .  $\lambda_Z^{ini} = \lambda_Z^{inv} = constant$  does not hold in Figure 3.

However the inversion property as such is exhibited by the curves of  $\lambda_Z^{ini}$ . From the first panel it is clear that there are curves that at a given  $\lambda_Z^{ini}$  exhibit pressure-induced shortening ( $d\lambda_Z(P) < 0$ ), subsequently pass through a point where they are locally vertical, that is  $d\lambda_Z(P) = 0$ , and continue with pressure-induced elongation ( $d\lambda_Z(P) > 0$ ). This means that Figure 3 suggests that instead  $\lambda_Z^{ini} = \lambda_Z^{inv} = constant$ , the model (7) has the inversion property in a sense that  $\lambda_Z^{inv} = \lambda_Z^{inv}(P, \lambda_Z^{ini})$ .

It leads us to a modified definition of  $\lambda_Z^{inv}$  which does not understand the inversion in the axial response of the tube as a global property holding for all inflating pressures. Rather we can understand it as a local property which  $\lambda_Z$ - $P$  curve may exhibit. Thus we say that  $\lambda_Z^{inv}$  is not a line in  $\lambda_Z$ - $P$  graph but it is a point on  $\lambda_Z$ - $P$  graph, where the tangent made to the graph is vertical. This is in contrast to [17, 30, 40] where inversion is strictly understood as the line separating  $\lambda_Z$ - $P$  curves with respect to a monotony. Here presented relaxation of the definition exactly corresponds to accepting roots of (18) that are not independent of  $\lambda_\Theta$  as is discussed in [40]. Proposed relaxation could be of particular interest in research where the inflation-extension response of a tube is studied with respect to a certain interval of pressures. Arteries are a good example, because their mechanical response at a pressure that falls into an interval bounded with diastole and systolic, is clinically the most relevant.

## 7. Conclusion

This study dealt with an effect of the axial prestretch on the mechanical response of thin-walled tubes. Previous results showing that a prestretched tube may exhibit axial inversion, were extended with a finding that the same prestretch also leads to maximization of a volume accommodated in the tube. From known strain energy density functions, the Mooney-Rivlin and Gent models were proved to have this property. The inversion in axial deformation of the HGO model for the human abdominal aorta was also studied. It was found that the inversion in a form of a line, that would separate  $\lambda_z$ - $P$  graph into pressure-induced elongation and pressure-induced shortening, does not exist in this case. However, when this property was studied from a local point of view,  $F_{red} = \text{constant}$  responses exhibited inversion points that depended on applied pressure. Numerical results showed that these local inversion points correspond to states of maximal internal volume of a pressurized tube.

## Acknowledgement

This study has been supported by the Czech Science Foundation in project 18-26041S entitled "Effect of axial prestretch on the mechanical response of nonlinearly elastic and viscoelastic tubes".

## References

- [1] J.D. Humphrey, Cardiovascular solid mechanics: Cells, tissues, and organs, Springer-Verlag, New York, 2002.
- [2] P. Kalita, R. Schaefer, Mechanical Models of Artery Walls, Arch. Comput. Method Eng. 15 (2008) 1-36. <https://doi.org/10.1007/s11831-007-9015-5>
- [3] L. Horný, M. Netušil, T. Voňavková, Axial Prestretch and Circumferential Distensibility in Biomechanics of Abdominal Aorta, Biomech. Model. Mechanobiol. 13 (2014) 783-799. <https://doi.org/10.1007/s10237-013-0534-8>.
- [4] H-C. Han, Y.C. Fung, Longitudinal Strain of Canine and Porcine Aortas, J. Biomech. 28 (1995) 637-641. [https://doi.org/10.1016/0021-9290\(94\)00091-H](https://doi.org/10.1016/0021-9290(94)00091-H).
- [5] D.H. Bergel, The Static Elastic Properties of the Arterial Wall, J. Physiol. 156 (1961) 445-457. <https://doi.org/10.1113/jphysiol.1961.sp006686>.
- [6] L. Horny, T. Adamek, E. Gultova, R. Zitny, J. Vesely, H. Chlup, and S. Konvickova, Correlations between Age, Prestrain, Diameter and Atherosclerosis in the Male Abdominal Aorta, J. Mechan. Behav. Biomed. Mater. 4 (2011) 2128-2132. <https://doi.org/10.1016/j.jmbbm.2011.07.011>.
- [7] L. Horný, T. Adámek, M. Kulvajtová, A Comparison of Age-Related Changes in Axial Prestretch in Human Carotid Arteries and in Human Abdominal Aorta, Biomech. Model. Mechanobiol. 16 (2017) 375-383. <https://doi.org/10.1007/s10237-016-0797-y>.
- [8] L. Horny, T. Adamek, M. Kulvajtova, Analysis of Axial Prestretch in the Abdominal Aorta with Reference to Post Mortem Interval and Degree of Atherosclerosis, J. Mechan. Behav. Biomed. Mater. 33 (2014) 93-98. <https://doi.org/10.1016/j.jmbbm.2013.01.033>.
- [9] A. Kamenskiy, A. Seas, G. Bowen, P. Deegan, A. Desyatova, N. Bohlim, W. Poulson, J. Mactaggart, In Situ Longitudinal Pre-Stretch in the Human Femoropopliteal Artery, Acta Biomater. 32 (2016) 231-237. <https://doi.org/10.1016/j.actbio.2016.01.002>.
- [10] A.V. Kamenskiy, I. I. Pipinos, Y.A. Dzenis, N.Y. Phillips, A.S. Desyatova, J. Kitson, R. Bowen, J.N. MacTaggart, Effects of Age on the Physiological and Mechanical Characteristics of Human Femoropopliteal Arteries, Acta Biomater. 11 (2015) 304-313. <https://doi.org/10.1016/j.actbio.2014.09.050>.
- [11] C.A.J. Schulze-Bauer, C. Mörth, G.A. Holzapfel, Passive Biaxial Mechanical Response of Aged Human Iliac Arteries, J. Biomech. Eng. 125 (2003) 395-406. <https://doi.org/10.1115/1.1574331>.

- [12] L. Horny, T. Adamek, R. Zitny, Age-Related Changes in Longitudinal Prestress in Human Abdominal Aorta, *Arch. Appl. Mech.* 83 (2013) 875-888. <https://doi.org/10.1007/s00419-012-0723-4>.
- [13] P. Van Loon, W. Klip, E.L. Bradley, Length-Force and Volume-Pressure Relationships of Arteries, *Biorheology* 14 (1977) 181-201. <https://doi.org/10.3233/BIR-1977-14405>.
- [14] H. Weizsäcker, H. Lambert, K. Pascale, Analysis of the Passive Mechanical Properties of Rat Carotid Arteries, *J. Biomech.* 16 (1983) 703-715. [https://doi.org/10.1016/0021-9290\(83\)90080-5](https://doi.org/10.1016/0021-9290(83)90080-5).
- [15] P.B. Dobrin, Biaxial Anisotropy of Dog Carotid Artery: Estimation of Circumferential Elastic Modulus, *J. Biomech.* 19 (1986) 351-358. [https://doi.org/10.1016/0021-9290\(86\)90011-4](https://doi.org/10.1016/0021-9290(86)90011-4).
- [16] K. Takamizawa, K. Hayashi, Strain Energy Density Function and Uniform Strain Hypothesis for Arterial Mechanics, *J. Biomech.* 20 (1987) 7-17. [https://doi.org/10.1016/0021-9290\(87\)90262-4](https://doi.org/10.1016/0021-9290(87)90262-4).
- [17] R.W. Ogden, C.A.J. Schulze-Bauer, Phenomenological and Structural Aspects of the Mechanical Response of Arteries, in: J. Casey, G. Bao (Eds.), *Mechanics in Biology*, American Society of Mechanical Engineers, Applied Mechanics Division, New York, 2000, pp. 125-140.
- [18] G. Sommer, P. Regitnig, L. Költringer, G.A. Holzapfel. Biaxial Mechanical Properties of Intact and Layer-Dissected Human Carotid Arteries at Physiological and Supraphysiological Loadings, *Am. J. Physiol. - Heart Circ. Physiol.* 298 (2010) H898-H912. <https://doi.org/10.1152/ajpheart.00378.2009>.
- [19] A.N. Gent, A New Constitutive Relation for Rubber, *Rubber Chem. Technol.* 69 (1996) 59-61. <https://doi.org/10.5254/1.3538357>.
- [20] C.O. Horgan, G. Saccomandi, A Molecular-Statistical Basis for the Gent Constitutive Model of Rubber Elasticity, *J. Elast.* 68 (2002): 167-176. <https://doi.org/10.1023/A:1026029111723>.
- [21] L.M. Kanner, C.O. Horgan, Elastic Instabilities for Strain-Stiffening Rubber-Like Spherical and Cylindrical Thin Shells Under Inflation, *Int. J. Non-Lin. Mech.* 42 (2007) 204-215. <https://doi.org/10.1016/j.ijnonlinmec.2006.10.010>.
- [22] L. Horný, M. Netušil, M. Daniel, Limiting Extensibility Constitutive Model with Distributed Fibre Orientations and Ageing of Abdominal Aorta, *J. Mechan. Behav. Biomed. Mater.* 38 (2014) 39-51. <https://doi.org/10.1016/j.jmbbm.2014.05.021>.
- [23] G. Marckmann, E. Verron, Comparison of Hyperelastic Models for Rubber-Like Materials, *Rubber Chem. Technol.* 79 (2006) 835-858. <http://doi.org/10.5254/1.3547969>.
- [24] G.A. Holzapfel, T.C. Gasser, R.W. Ogden, A New Constitutive Framework for Arterial Wall Mechanics and a Comparative Study of Material Models, *J. Elast.* 61 (2000): 1-48. <https://doi.org/10.1023/A:1010835316564>.
- [25] T.C. Gasser, R.W. Ogden, G.A. Holzapfel, Hyperelastic Modelling of Arterial Layers with Distributed Collagen Fibre Orientations, *J. Roy. Soc. Interface* 3 (2006) 15-35. <https://doi.org/10.1098/rsif.2005.0073>.
- [26] L. Horný, M. Netušil, Z. Horák, Limit Point Instability in Pressurization of Anisotropic Finitely Extensible Hyperelastic Thin-Walled Tube, *Int. J. Non-Lin. Mech.* 77 (2015) 107-114. <https://doi.org/10.1016/j.ijnonlinmec.2015.08.003>.
- [27] A.N. Gent, Elastic Instabilities in Rubber, *Int. J. Non-Lin. Mech.* 40 (2005) 165-175. <https://doi.org/10.1016/j.ijnonlinmec.2004.05.006>.
- [28] L.M. Kanner, C. O. Horgan, Elastic Instabilities for Strain-Stiffening Rubber-Like Spherical and Cylindrical Thin Shells Under Inflation, *Int. J. Non-Lin. Mech.* 42 (2007) 204-215. <https://doi.org/10.1016/j.ijnonlinmec.2006.10.010>.
- [29] L. Horný, M. Netušil, How does Axial Prestretching Change the Mechanical Response of Nonlinearly Elastic Incompressible Thin-Walled Tubes, *Int. J. Mech. Sci.* 106 (2016) 95-106. <https://doi.org/10.1016/j.jimecsci.2015.08.014>.
- [30] C.O. Horgan, G. Saccomandi, A description of arterial wall mechanics using limiting chain extensibility constitutive models, *Biomech. Model. Mechanobiol.* 1 (2003) 251-266. <https://doi.org/10.1007/s10237-002-0022-z>
- [31] S. Kyriakides, C. Yu-Chung, On the Inflation of a Long Elastic Tube in the Presence of Axial Load, *Int. J. Solids Struct.* 26 (1990) 975-991. [https://doi.org/10.1016/0020-7683\(90\)90012-K](https://doi.org/10.1016/0020-7683(90)90012-K).

- [32] S. Kyriakides, C. Yu-Chung, The Initiation and Propagation of a Localized Instability in an Inflated Elastic Tube, *Int. J. Solids Struct.* 27 (1991) 1085-1111. [https://doi.org/10.1016/0020-7683\(91\)90113-T](https://doi.org/10.1016/0020-7683(91)90113-T).
- [33] S. Pearce, Effect of Strain-Energy Function and Axial Prestretch on the Bulges, Necks and Kinks Forming in Elastic Membrane Tubes, *Math. Mech. Solids* 17 (2012) 860-875. <https://doi.org/10.1177/1081286511433084>.
- [34] A.V. Kamenskiy, Y.A. Dzenis, S.A.J. Kazmi, M.A. Pemberton, I.I. Pipinos, N.Y. Phillips, K. Herber, T. Woodford, R.E. Bowen, C.S. Lomneth, J.N. MacTaggart, Biaxial Mechanical Properties of the Human Thoracic and Abdominal Aorta, Common Carotid, Subclavian, Renal and Common Iliac Arteries, *Biomech. Model. Mechanobiol.* 13 (2014): 1341-1359. <https://doi.org/10.1007/s10237-014-0576-6>.
- [35] W. Wan, J.B. Dixon, R.L. Gleason, Constitutive modeling of mouse carotid arteries using experimentally measured microstructural parameters, *Biophysical J.* 102 (2012) 2916-2925. <https://doi.org/10.1016/j.bpj.2012.04.035>
- [36] M. Jadidi, M. Habibnezhad, E. Anttila, K. Maleckis, A. Desyatova, J. MacTaggart, A. Kamenskiy, Mechanical and structural changes in human thoracic aortas with age, *Acta Biomater.* 103 (2020) 172-188. <https://doi.org/10.1016/j.actbio.2019.12.024>
- [37] Q. Liu, Q. Wen, M. Mottahedi, H. - C. Han, Artery buckling analysis using a four-fiber wall model. *J. Biomech.* 47 (2014) 2790-2796. <https://doi.org/10.1016/j.jbiomech.2014.06.005>
- [38] T. Matsumoto, K. Hayashi, Stress and strain distribution in hypertensive and normotensive rat aorta considering residual strain, *J. Biomech. Eng.* 118 (1996) 62-73. <https://doi.org/10.1115/1.2795947>
- [39] L. Horný, Axial prestretch and biomechanics of abdominal aorta, Habilitation thesis, Czech Technical University in Prague, 2015. <http://users.fs.cvut.cz/~hornyluk/files/Horny-L-Habilitation-thesis-Axial-prestretch-and-biomechanics-of-aorta-2015.pdf>
- [40] R. W. Ogden, G. Saccomandi, Introducing mesoscopic information into constitutive equations for arterial walls. *Biomech. Model. Mechanobiol.* 6(2007) 333-344. <https://doi.org/10.1007/s10237-006-0064-8>
- [41] R. W. Ogden, Anisotropy and nonlinear elasticity in arterial wall mechanics, in: *Biomechanical modelling at molecular, cellular and tissue levels*, CISM International Centre for Mechanical Sciences, Courses and Lectures, 508 (2009) 179-258. [https://doi.org/10.1007/978-3-211-95875-9\\_3](https://doi.org/10.1007/978-3-211-95875-9_3)
- [42] R. W. Ogden, Nonlinear elasticity with applications to soft fibre-reinforced materials, in: L. Dorfmann, R. W. Ogden (Eds.), *Nonlinear mechanics of soft fibrous materials*, CISM International Centre for Mechanical Sciences, Courses and Lectures, 559 (2015) 1-48. [https://doi.org/10.1007/978-3-7091-1838-2\\_1](https://doi.org/10.1007/978-3-7091-1838-2_1)